

VU Research Portal

A role for icebergs in the 8.2 ka climate event

Wiersma, A.P.; Jongma, J.I.

published in

Climate Dynamics

2009

DOI (link to publisher)

[10.1007/s00382-009-0645-1](https://doi.org/10.1007/s00382-009-0645-1)

document version

Publisher's PDF, also known as Version of record

[Link to publication in VU Research Portal](#)

citation for published version (APA)

Wiersma, A. P., & Jongma, J. I. (2009). A role for icebergs in the 8.2 ka climate event. *Climate Dynamics*.
<https://doi.org/10.1007/s00382-009-0645-1>

General rights

Copyright and moral rights for the publications made accessible in the public portal are retained by the authors and/or other copyright owners and it is a condition of accessing publications that users recognise and abide by the legal requirements associated with these rights.

- Users may download and print one copy of any publication from the public portal for the purpose of private study or research.
- You may not further distribute the material or use it for any profit-making activity or commercial gain
- You may freely distribute the URL identifying the publication in the public portal ?

Take down policy

If you believe that this document breaches copyright please contact us providing details, and we will remove access to the work immediately and investigate your claim.

E-mail address:

vuresearchportal.ub@vu.nl

A role for icebergs in the 8.2 ka climate event

Ane P. Wiersma · Jochem I. Jongma

Received: 30 December 2008 / Accepted: 31 July 2009 / Published online: 23 August 2009
© The Author(s) 2009. This article is published with open access at Springerlink.com

Abstract We investigate the potential role of icebergs in the 8.2 ka climate event, using a coupled climate model equipped with an iceberg component. First, we evaluate the effect of a large iceberg discharge originating from the decaying Laurentide ice sheet on ocean circulation, compared to a release of an identical volume of freshwater alone. Our results show that, on top of the freshwater effect, a large iceberg discharge facilitates sea-ice growth as a result of lower sea-surface temperatures induced by latent heat of melting. This causes an 8% increased sea-ice cover, 5% stronger reduction in North Atlantic Deep Water production and 1°C lower temperature in Greenland. Second, we use the model to investigate the effect of a hypothetical two-stage lake drainage, which is suggested by several investigators to have triggered the 8.2 ka climate event. To account for the final collapse of the ice-dam holding the Laurentide Lakes we accompany the secondary freshwater pulse in one scenario with a fast 5-year iceberg discharge and in a second scenario with a slow 100-year iceberg discharge. Our experiments show that a two-stage lake drainage accompanied by the collapsing ice-dam could explain the anomalies observed around the 8.2 ka climate event in various climate records. In addition, they advocate a potential role for icebergs in the 8.2 ka climate

event and illustrate the importance of latent heat of melting in the simulation of climate events that involve icebergs. Our two-stage lake drainage experiments provide a framework in the discussion of two-stage lake drainage and ice sheet collapse.

Keywords 8.2 ka event · Climate modeling · Icebergs · Laurentide ice sheet · Hudson Strait · Holocene · Heinrich events

1 Introduction

The 8.2 ka climate event is a 160-year cold and dry period centered around 8,200 years ago in the Greenland ice core records where it is the most pronounced Holocene climate event (Alley et al. 1997). Outside of Greenland, the 8.2 ka climate event is recorded in a large number of proxy archives in the North Atlantic area and in areas influenced by monsoons (Alley and Ágústóttir 2005; Rohling and Pälike 2005; Wiersma and Renssen 2006).

The proposed cause of the event is the sudden drainage of the Laurentide lakes (Lake Agassiz and Ojibway) around 8,470 years BP through the Hudson Strait triggered by the early Holocene decay of the remnants of the Laurentide ice sheet (Barber et al. 1999). The resulting freshening of surface waters inhibited deep-water formation in the North Atlantic Ocean, leading to a decrease in northward oceanic heat transport and cooler conditions. Climate model experiments successfully simulated such a mechanism (e.g., Renssen et al. 2001, 2002; Bauer et al. 2004; LeGrande et al. 2006; Wiersma et al. 2006).

Although the proposed mechanism of lake drainage is consistent with many of the observed patterns (Alley and Ágústóttir 2005; Wiersma and Renssen 2006), the

A. P. Wiersma · J. I. Jongma
Faculty of Earth and Life Sciences,
Vrije Universiteit Amsterdam, De Boelelaan 1085,
1081 HV Amsterdam, The Netherlands
e-mail: jochem.jongma@falw.vu.nl

A. P. Wiersma (✉)
Department of Morphology and Sedimentary Systems,
Deltares, Princetonlaan 6, 3584 CB Utrecht, The Netherlands
e-mail: ane.wiersma@deltares.nl

hypothesis is not without debate. For instance, the red clay-layer in the Hudson Strait deposited by the lake outburst (Kerwin 1996) was dated at 8470 ± 300 (1σ) cal. year BP (Barber et al. 1999), while the start of the climate event was dated at $8,247 \pm 47$ cal. year BP in Greenland ice cores (Thomas et al. 2007; Rasmussen et al. 2006). Thus, although these events could coincide considering dating uncertainties, the lake outburst possibly predates the start of the event by more than 200 years. Another matter of debate is that lake level reconstructions as well as the sedimentological signature of the lake drainage suggest that a single lake outburst could be an oversimplification, and the lakes may have drained in two separate outbursts (Teller et al. 2002; Hillaire-Marcel et al. 2007). This is also suggested by the two-peaked nature of the event as suggested by several high-resolution North Atlantic deep-sea sediment cores (e.g., Ellison et al. 2006; Flesche-Kleiven et al. 2008). In Ellison et al. (2006), additional support for a two-stage drainage comes from two reconstructed periods of surface ocean freshening which are separated by 200 years (Fig. 1): the first one correlated with the lake outburst at 8,470 yr BP (Barber et al. 1999) and the second one correlated with the cooling in Greenland.

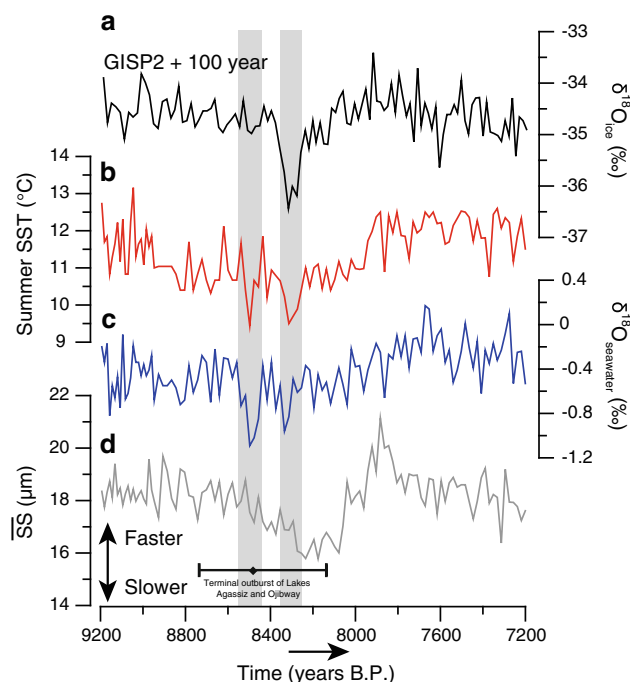


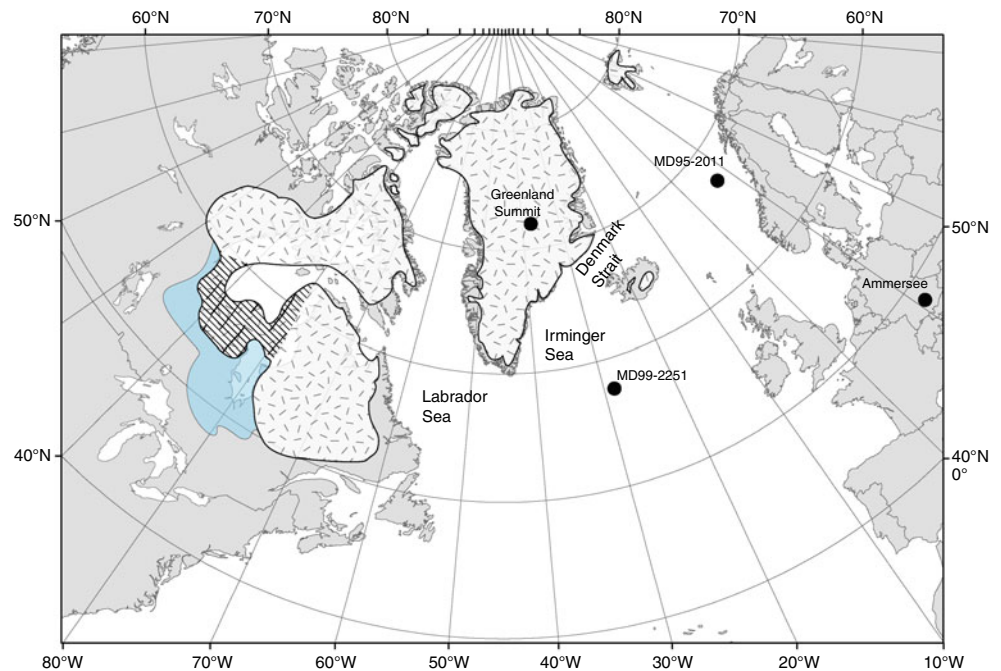
Fig. 1 Inferred surface and deep ocean properties in core MD99-2251 (Ellison et al. 2006) compared to the GISP2 ice core. **a** GISP2 temperature ($\delta^{18}\text{O}_{\text{ice}}$) record with a constant age offset of +100 years as applied by Ellison et al. (2006). **b** Faunal derived transfer function estimates of summer SSTs in MD99-2251. **c** Inferred surface ocean stable isotope composition ($\delta^{18}\text{O}_{\text{seawater}}$) in MD99-2251. **d** Variations in the mean size of the sortable silt as indicator of the near-bottom flow speed. The diamond marks the estimated timing of the final lake outburst at 8470 cal. ka BP (Barber et al. 1999) with 1σ uncertainty bars

In addition to the draining of the Laurentide Lakes, freshwater could also have been supplied in the form of icebergs by the decaying Laurentide ice sheet. After all, in the period around the 8.2 ka climate event the ice-dam that blocked the Laurentide Lakes (Fig. 2) disappeared fast, according to reconstructions by Dyke (2004) within a period of 200 years, and increased ice-rafted debris (IRD) concentrations and iceberg scours suggest increased iceberg activity in this period (Bond et al. 1997, 2001; Moros et al. 2004; Josenhans and Zevenhuizen 1990; Lajeunesse and St-Onge 2008; Jakobsson 2008).

In a previous modeling study on the 8.2 ka climate event, Wiersma et al. (2006) accounted for this additional freshwater source in the form of icebergs by releasing various volumes freshwater exceeding the estimated lake volume of $1.63 \times 10^{14} \text{ m}^3$ (Leverington et al. 2002). However, in that study, iceberg dynamics and thermodynamics were not accounted for. Icebergs distribute freshwater over large distances and influence the surface ocean in two distinct ways: (1) they freshen the surface water through melting and (2) they cool the ocean as latent heat, which is required to melt the ice, is extracted from the surrounding waters. Through these mechanisms they facilitate the formation of sea-ice (Jongma et al. 2009), which can affect deepwater formation in various ways.

In this study, we use the 8.2 ka event as a case study to test the sensitivity of the early Holocene North Atlantic ocean circulation to a perturbation by an iceberg discharge released near the Hudson Strait outlet. For this purpose we use the ECBilt-CLIO-VECODE coupled climate model (Goosse and Fichefet 1999) equipped with a dynamical/thermodynamical iceberg component (Jongma et al. 2009). First, we evaluate the effect on ocean circulation of a perturbation by a large iceberg discharge in comparison to a perturbation by freshwater alone (Wiersma et al. 2006). Second, we study the effect of a hypothetical two-stage lake drainage with the second lake drainage accompanied by an iceberg discharge representing the partial collapse of the Laurentide ice sheet, using the following strategy: our estimates of fresh water volumes (Teller et al. 2002), time-interval between the two stages (Ellison et al. 2006), and iceberg discharge volume (Dyke 2004) are consistent with reconstructions. However, since there are large uncertainties in the decay rate of the ice sheet, we experiment with a fast (5-year) and a slow (100-year) collapse of the ice sheet, the latter belonging to the lower range of decay rates of this part of the ice-dam according to ice-sheet reconstructions (Dyke 2004). This results in two separate experiments, which are identical except for the duration of the iceberg discharge representing the ice-sheet decay accompanying the second lake drainage. The outcomes of these hypothetical experiments are compared to independent climate reconstructions (e.g., Ellison et al. 2006;

Fig. 2 Remnants of the Laurentide ice sheet and proglacial lakes Agassiz and Ojibway at 7.7 ^{14}C ka BP (~ 8.5 cal. ka BP), just before the 8.2 ka climate event (Dyke 2004). The lakes have a combined freshwater volume of $1.63 \times 10^{14} \text{ m}^3$. The ice-dam (shaded part of the ice sheet), that we calculated to contain at least $1.0 \times 10^{14} \text{ m}^3$ of freshwater equivalent ice, had disappeared by 7.6 ^{14}C ka BP (~ 8.4 cal. ka BP) (Dyke 2004). Locations of sites and relevant areas that will be discussed in this paper (Figs. 8, 9) are also indicated



von Grafenstein et al. 1998; Risebrobakken et al. 2003), in order to test whether a scenario of two-stage lake drainage can explain climate anomalies around the 8.2 ka event. Results from these experiments are meant to serve as a framework in the discussion of a two-stage lake drainage triggering the 8.2 ka climate event and climate anomalies around it.

2 Methods

2.1 Climate model

ECBilt-CLIO-VECODE (version 3) is a global, three-dimensional climate model of intermediate complexity consisting of an atmospheric (ECBilt), sea-ice-ocean (CLIO) and vegetation component (VECODE). CLIO (Goosse and Fichefet 1999) is a primitive equation, free-surface ocean general circulation model (OGCM) (Deleersnijder and Campin 1995; Campin and Goosse 1999) coupled to a comprehensive sea-ice model with a representation of both thermodynamic and dynamic processes (Fichefet and Morales Maqueda 1997; Goosse and Fichefet 1999). The horizontal resolution of CLIO is 3° longitude by 3° latitude and there are 20 unequally spaced vertical levels in the ocean. ECBilt (Opsteegh et al. 1998) is a spectral quasi-geostrophic atmospheric model with three levels and a T-21 resolution ($\sim 5.6^\circ$ lat. \times 5.6° lon.). The pre-industrial overturning strength in CLIO in the North Atlantic of ~ 27 Sv is close to present day estimates of 23 ± 3 Sv (Ganachaud and Wunsch 2000). VECODE (Brovkin et al.

2002) is a dynamic global vegetation model that simulates dynamics of two main terrestrial plant functional types (trees and grasses) as well as desert (bare soil). More information about ECBilt-CLIO-VECODE and its climatology can be found on the models' website (<http://www.knmi.nl/onderzk/CKO/ecbilt.html>).

2.2 Iceberg model

2.2.1 Iceberg dynamics

The dynamics and thermodynamics of our interactively coupled iceberg module (Jongma et al. 2009) are based on the iceberg-drift model described by Bigg et al. (1997) and Gladstone et al. (2001). This model calculates the path of an iceberg as a function of the Coriolis force, air drag, water drag, sea-ice drag, horizontal pressure gradient force and wave radiation force. The general drag relations and the wave radiation force are according to Smith (1993). Relevant forcing variables from the atmosphere- and ocean model are linearly interpolated from the four neighboring grid-corners.

In earlier studies (e.g., Watkins et al. 2007; Jongma et al. 2009), iceberg grounding is treated by fixing the icebergs position when the iceberg enters a shallow grid cell, until it melts enough to float again. In this study we introduce a weak orthogonal repulsion (0.003 m/s) of icebergs that are about to get grounded, to mimic tidal action. This almost immobilizes the grounding icebergs, while allowing changing winds and currents to move the icebergs to deeper waters.

2.2.2 Iceberg thermodynamics

Iceberg melting is simplified to basal melt, lateral melt and wave erosion (Bigg et al. 1997). Melting at the base occurs through turbulent heat transfer as a function of the temperature difference between iceberg (-4°C) and surrounding water, and the relative motion of the water past the iceberg that acts to carry heat to the berg (Weeks and Campbell 1973). Melting along the sides occurs through buoyant convection as a function of water temperature (El-Tahan et al. 1987), and wave erosion as a function of sea roughness (Bigg et al. 1997). To simulate a damping effect of sea-ice on sea roughness we introduced a simple dependence of sea roughness on sea-ice, proportional to the fraction of open water in the sea-ice cover. The icebergs roll over when the height of the iceberg is not stable with its length (Weeks and Mellor 1978), but after rolling over they remain tabular and maintain their constant length-to-width ratio of 1.5:1.

The freshwater and latent heat flux associated with the melting icebergs are fed back to the local grid-cell in the ocean model. The heat involved in the phase-transition from ice to water ($3.34 \times 10^5 \text{ J kg}^{-1}$ at 0°C) is around 80 times higher than the heat involved in raising the temperature of the same volume of water by 1°C . Given the large iceberg discharges, the iceberg model was upgraded by adding basal and lateral fluxes of freshwater and latent heat to the respective ocean layer, instead of adding these fluxes to the ocean surface (Jongma et al. 2009). Possible feedbacks from the icebergs to the atmosphere, such as the effect on winds, air humidity or surface albedo are not taken into account. Given the observational uncertainties and the limited model-resolution, the iceberg model coupled to ECBilt-CLIO-VECODE simulates a reasonable present-day iceberg distribution (Jongma et al. 2009). However, please note that in our model icebergs enter the Mediterranean Sea through a Gibraltar Strait that is much larger than in reality.

2.3 Experimental setup

2.3.1 Model boundary conditions

The experiments were started from a quasi-equilibrium early Holocene climate state identical to that described in Wiersma et al. (2006). Atmospheric greenhouse gas concentrations (Raynaud et al. 2000) and orbital parameters (Berger and Loutre 1991; Berger 1992) in the climate model are set to 8.5 ka BP values. In addition we allowed for a remnant Laurentide ice sheet by adjusting surface albedo and elevation of the concerning grid-cells according to the Peltier (1994) reconstruction. To represent the background Laurentide ice sheet melting in the early

Holocene, we introduced a baseline flow (Bauer et al. 2004) of 0.172 Sv ($1 \text{ Sv} = 10^6 \text{ m}^3/\text{s}$) (Licciardi et al. 1999) into the Labrador Sea during the full course of the experiments, starting 400 years before the perturbations. This baseline flow leads to strongly reduced deep-water formation in the Labrador Sea (Wiersma et al. 2006) in agreement with proxy-data (Hillaire-Marcel et al. 2001). In addition, the baseline flow results in reduced North Atlantic overturning and a shallower NADW cell in the early Holocene control climate, but overturning in the Nordic Seas remains almost unaffected. In response to a freshwater pulse representing the lake drainage causing the 8.2 ka climate event, experiments with a baseline flow showed a slower recovery of the overturning circulation than experiments without a baseline flow (Wiersma et al. 2006).

2.3.2 Setup of the sensitivity experiment

In the early Holocene climate state we introduce an armada of icebergs in the Labrador Sea with an ice volume of $1.77 \times 10^{14} \text{ m}^3$, equivalent to a freshwater volume of $1.63 \times 10^{14} \text{ m}^3$. This latter value is the estimated volume of the Laurentide Lakes (Leverington et al. 2002), and is identical to the volume of freshwater released in several previous freshwater perturbation modeling studies of the 8.2 ka climate event (Bauer et al. 2004; LeGrande et al. 2006; Wiersma et al. 2006). The iceberg discharge consists of ten classes of icebergs identical to Bigg et al. (1997) (Table 1), based on present-day observations of icebergs in the Arctic (Dowdeswell et al. 1992) (Fig. 3).

The iceberg discharge is released regularly every day over a 5-year period at five release sites near the Hudson Strait outlet. The experiment was performed five times (i.e., five ensemble members), each with different initial conditions that were obtained from a continuation of the early Holocene experiment and are spaced 10 years apart. From this point on the iceberg perturbation experiment will be referred to as IBP.

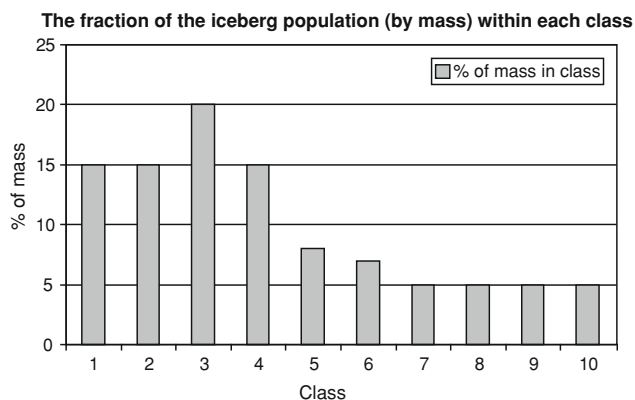
The iceberg discharge experiments are compared to freshwater perturbation experiments in which a freshwater pulse of $1.63 \times 10^{14} \text{ m}^3$ is released during 5 years into the Labrador Sea in an identical early Holocene climate. The experiment is described in detail in Wiersma et al. (2006) as EHBLF5, and also consists of five ensemble members. For convenience, in this study we will refer to this freshwater perturbation experiment as FWP.

2.3.3 Scenarios for two-stage lake drainage and ice-dam collapse

In the second part of this article we use the iceberg model to simulate two hypothetical scenarios for the circumstances leading to the 8.2 ka climate event. In these

Table 1 Fraction, size and weight of individual icebergs in each class

Size class	Fraction of population by mass (%) for Armada	Length (m)	Width (m)	Keel depth (m)	Freeboard (m)	Mass (10^9 kg)
1	15	100	67	67	10	0.475
2	15	200	133	133	20	3.719
3	20	300	200	200	30	12.6
4	15	400	267	267	40	30.0
5	8	500	333	300	45	52.6
6	7	600	400	300	45	75.9
7	5	750	500	300	45	118.5
8	5	900	600	300	45	170.7
9	5	1,200	800	300	45	303.5
10	5	1,500	1,000	300	45	474.2

**Fig. 3** Distribution of icebergs over the different classes, in agreement with observations from Weeks and Mellor (1978) and Dowdeswell et al. (1992)

scenarios a two-stage lake outburst is combined with a fast respectively a slow collapse of the ice-dam (Fig. 2). The two-stage lake outburst is based on the sequence of events observed in deep-sea sediment core MD99-2251 (Ellison et al. 2006) (Fig. 1), indicating two short periods of surface-ocean freshening and cooling separated by about 200 years (Fig. 1b, c). The timing of the first event coincides with the timing of the lake outburst as deduced by Barber et al. (1999) and with a longer term weakening of bottom current strength (Ellison et al. 2006), an indicator of overturning intensity (Fig. 1d). This event has no large-scale counterpart in the Greenland ice core records (Ellison et al. 2006). The second period of cooling and freshening is associated with the 8.2 ka BP cooling as observed in the Greenland ice cores (Fig. 1a), and coincides with the most pronounced weakening in bottom current strength (Ellison et al. 2006).

We prescribe a two-stage drainage of the Laurentide Lakes as inferred from lake level reconstructions by Teller et al. (2002), with a first stage drainage of 1.13×10^{14} km³ of freshwater, followed by a smaller outburst of

0.50×10^{14} m³. The two outbursts are separated by a 200-year gap, corresponding to the gap between the periods of freshening as observed in Ellison et al. (2006). Starting from the previously described early Holocene state, we release the volume of the first outburst into the Labrador Sea over a 5-year period (equivalent to a constant freshwater flux of 0.72 Sv), followed after 200 years by the freshwater volume of the second outburst over a 5-year period (equivalent to a constant freshwater flux of 0.32 Sv) (Table 2).

Coinciding with the second lake drainage, we introduce an iceberg discharge to account for the ice-dam that decayed fast around the time of the two-stage lake outburst, according to reconstructions within 200 years (Dyke 2004; Fig. 2). We estimated the volume of the ice-dam (Fig. 2) by multiplying the area between 55°N and 60°N and 90°W and 80°W (the estimated surface area) with an average height of the ice-dam of 340 m, amounting to 1.0×10^{14} m³ of freshwater equivalent. This volume is a conservative estimate given the maximum heights of the ice-dam in different cross-sections used by Clarke et al. (2004) that range from 340 m to 735 m. We convert the ice-dam volume into an iceberg discharge that is composed of the ten classes of icebergs illustrated in Table 1 and Fig. 3.

In the first two-stage lake drainage scenario (TS-5) we simulate an abrupt collapse of the ice-dam during the second lake drainage by introducing icebergs of the ice-dam volume over 5 years (Table 2). In the second two-stage lake drainage scenario (TS-100) we simulate a gradual decay of the ice-dam allowing for the longer time ranges given by Dyke (2004) by spreading the discharge over 100 years. We note that we apply a baseline flow simultaneously with the iceberg discharge, which already contains an ice melt runoff component. We consider this reasonable because the total volume of the iceberg discharge is minor ($\sim 3\%$), compared to the total runoff estimated in the 600-year period around the 8.2 ka climate

Table 2 Volume, release duration and timing of the two-stage lake drainage scenarios and of the iceberg discharge accompanying the second lake drainage

	First lake outburst ($t = 300$)	Second lake outburst ($t = 505$)	Iceberg discharge ($t = 505$)
TS-5	$1.13 \times 10^{14} \text{ m}^3$ in 5 years	$0.50 \times 10^{14} \text{ m}^3$ in 5 years	$1.00 \times 10^{14} \text{ m}^3$ in 5 years
TS-100	$1.13 \times 10^{14} \text{ m}^3$ in 5 years	$0.50 \times 10^{14} \text{ m}^3$ in 5 years	$1.00 \times 10^{14} \text{ m}^3$ in 100 years

In the background control climate that is perturbed, a baseline flow of 0.172 Sv is applied into the Labrador Sea

event (Licciardi et al. 1999) that underpins the 0.172 Sv baseline flow, and therefore the iceberg discharge should be interpreted as an acceleration in ice sheet decay. The TS-5 and TS-100 experiments were performed five times (i.e., five ensemble members). The initial conditions of the ensemble members were obtained from a continuation of the early Holocene experiment and are spaced 10 years apart.

3 Sensitivity experiments

3.1 Meltwater production and distribution in the IBP experiment

As soon as the icebergs are introduced near the Hudson Strait outlet they start distributing meltwater. When the daily release of icebergs stops, meltwater production gradually decreases for 2 years and continues in slower rates from that point (Fig. 4a). Peak melting takes place in summer, resulting from higher ocean temperatures. The distribution of meltwater by the icebergs (Fig. 4c) shows that most icebergs travel into the Atlantic Ocean where they are transported either northward along the Norwegian coast up to Spitsbergen, or southward within the North Atlantic subtropical gyre up to the Canary Islands. A fraction of the icebergs travels north after the release toward the Canadian Archipelago. There, larger icebergs cannot pass the shallow sills and first have to melt before they can enter the Arctic Ocean. As a result of perennial sea-ice cover and low temperatures in the Arctic Ocean and Baffin Bay, icebergs floating northward survive up to four decades. This explains the continuing meltwater production after most icebergs have melted during the first 7 years (Fig. 4a). The distribution of meltwater (and associated latent heat flux) over the different ocean layers (Fig. 4b) illustrates dominant melting in the upper ocean layer, due to a combination of wave-erosion being a dominant melting process and the fact that every iceberg is floating in this layer during its full life span. Because the upper ocean layer is also the thinnest layer (10 m), the relative cooling and freshening caused by the icebergs is even larger in this layer (84%). The melting icebergs trigger a distinct cooling

(Fig. 4d) of the surface ocean of up to 9°C in the release area near the Hudson Strait outlet gradually decreasing away from the release area. Although it is practically impossible to disentangle the primary cooling effect of the icebergs from secondary coupled climate interactions, the similarity of the temperature (Fig. 4d) and meltwater distribution (Fig. 4c) is striking.

The 7-year period in which the majority of the icebergs have melted (Fig. 4a) is comparably close to the 5-year freshwater introduction in the FWP experiment. Wiersma et al. (2006) showed that such a small difference in freshwater release duration does not lead to a different response of the ocean circulation in ECBilt-CLIO-VECODE in the case of identical freshwater volumes. To test whether the “tail” of meltwater production from surviving icebergs in the Arctic Ocean (Fig. 4a) influences our results, we performed a sensitivity experiment with no iceberg melt after the first 7 years, which revealed no marked difference compared to an experiment including the “tail” (not shown).

3.2 Ocean response and Greenland temperatures

Both the FWP and IBP experiment show an immediate decrease in North Atlantic Deep Water (NADW) formation (Fig. 5a, d) and an increase in total sea-ice area in the Northern Hemisphere (Fig. 5b, e) in response to the perturbations at $t = 100$. In response to the iceberg perturbation in IBP the average NADW exported southward decreases by $\sim 20\%$ from 11 Sv to 9 Sv after 70 years (Fig. 5a). The freshwater perturbation in FWP results in a more moderate response of less than $\sim 15\%$ (Fig. 5d). Although the magnitude of the response is different, the total duration of significantly weakened overturning is ~ 210 years in both experiments (Fig. 5a, d). In our model, oceanic heat transport correlates to NADW export, and also shows a decrease by $\sim 20\%$ in IBP, and by $\sim 15\%$ in FWP.

After the iceberg perturbation (IBP), the average sea-ice area in the Northern Hemisphere rapidly expands by 14% from $11.5 \times 10^{12} \text{ m}^2$ to $13.3 \times 10^{12} \text{ m}^2$, before rapidly retreating to normal values again after 15 years (Fig. 5b). From this point, average sea-ice area increases again to $12.7 \times 10^{12} \text{ m}^2$ followed by a gradual return to pre-perturbed values within 160 years after the perturbation. The

Fig. 4 Meltwater production and distribution in the IBP sensitivity experiment: **a** Monthly meltwater production by icebergs. The icebergs are released during the first 5 years. **b** Distribution of meltwater over the uppermost ten ocean model layers accumulated by the end of the fifth year, in percentage of total meltwater volume. **c** Meltwater volume from icebergs per grid cell accumulated by the end of the fifth year. The *solid arrows* indicate the main pathways, *stippled arrows* the minor pathways. **d** Mean annual sea surface temperature (SST) anomaly during the 5 years of iceberg release with respect to the equilibrium climate

freshwater perturbation on the other hand leads to an initial increase of 6% from $11.5 \times 10^{12} \text{ m}^3$ to $12.2 \times 10^{12} \text{ m}^3$ in average sea-ice area, followed by a drop toward $11.0 \times 10^{12} \text{ m}^3$ (Fig. 5e). After this drop below equilibrium values, average sea-ice cover increases again to $12.3 \times 10^{12} \text{ m}^3$ followed by a gradual retreat within 150 years after the freshwater pulse.

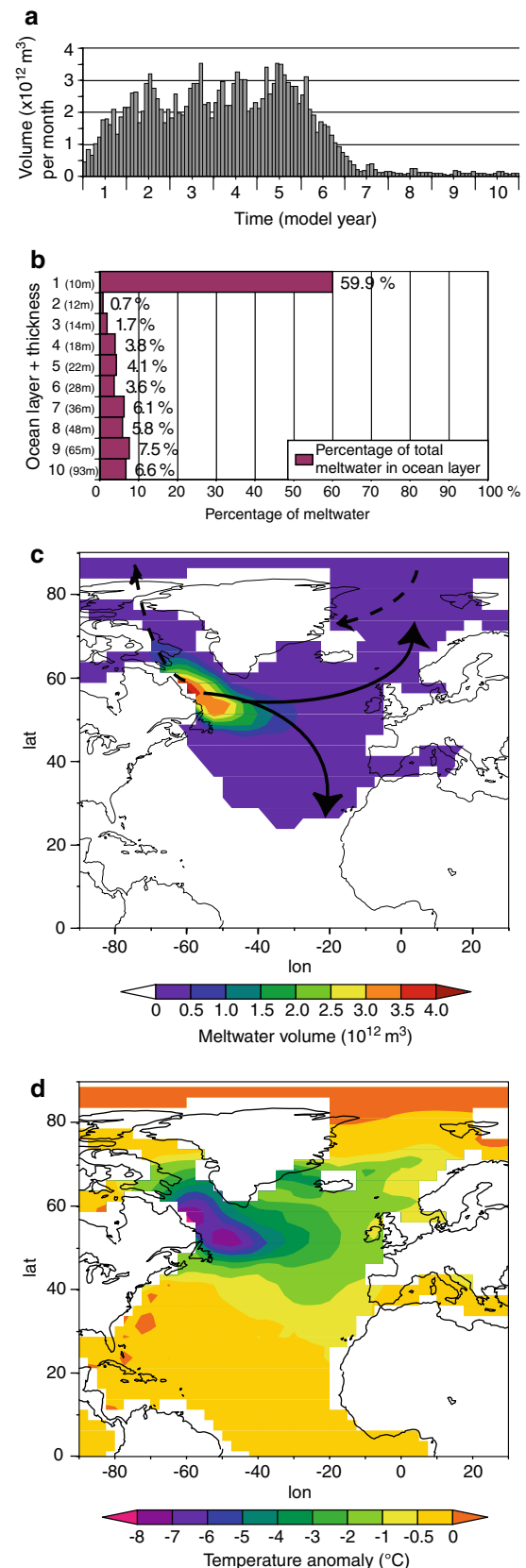
All ensemble members show a similar evolution in NADW production and sea-ice area in the Northern Hemisphere, which suggests that the perturbation by the icebergs and the freshwater that we apply does not bring the system into an intermediately stable state. As such, both perturbations lead to a generally predictable response of North Atlantic Ocean circulation.

At Greenland summit, simulated average temperatures abruptly drop by $\sim 3^\circ\text{C}$ in the IBP experiment (Fig. 5c) and $\sim 2^\circ\text{C}$ in the FWP experiment (Fig. 5f), followed by a fast return to pre-perturbed values, or even past pre-perturbed values in the FWP scenario. These decadal-scale temperature variations inversely resemble the variations in sea-ice area. In IBP, Greenland Summit ensemble average temperatures then drop sharply again by 2.5°C , recovering gradually in around 180 years after the perturbation (Fig. 5c). In FWP, this secondary cooling, with an ensemble average anomaly of up to 1.9°C lasts at least 80 years and possibly up to 190 years (Fig. 5f).

3.3 Spatial response

The perturbations by both the iceberg armada and the freshwater pulse lead to decreased deep-ocean convection, cooler sea surface temperatures (SST) in the North Atlantic Ocean and increased sea-ice cover. The major expansion of sea-ice area during the first 10 years of both perturbations (Fig. 5b, e) reflects a southward shift of the sea-ice edge, mainly in the Labrador Sea and Irminger Sea (Fig. 6). The larger sea-ice area in the IBP experiment is almost exclusively caused by a sea-ice tongue in the Labrador Sea (Fig. 6) following the contours of the main iceberg meltwater distribution and cooling (Fig. 4c, d).

In the perturbed state, between 125 and 200 model years, the IBP experiment shows a more pronounced



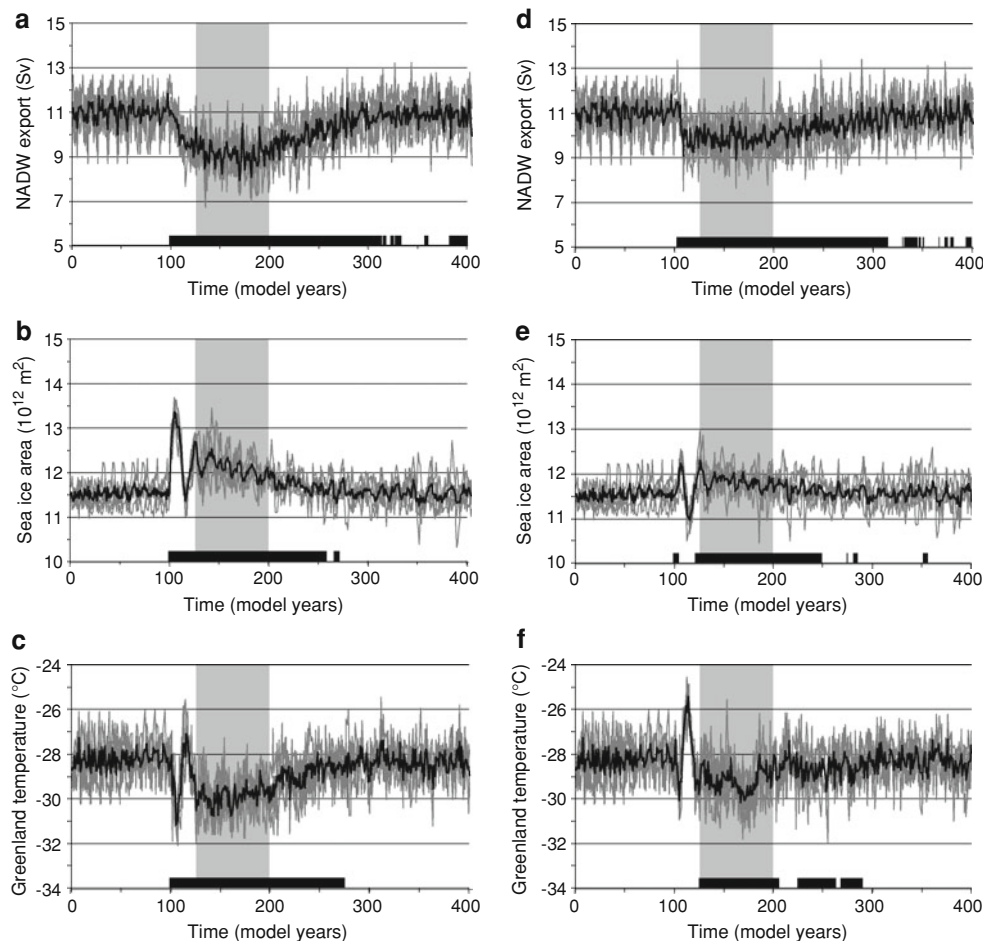


Fig. 5 Climatic response to the iceberg (IBP, *left panel*) and the freshwater (FWP; *right panel*) discharges, which start at $t = 100$. **a, d** North Atlantic Deep Water (NADW) exported southward in the Atlantic at 20°S . **b, e** Sea-ice area in the Northern Hemisphere. **c, f** Greenland summit annual temperatures where both GRIP and GISP2 ice cores are located. *Black lines* represent the ensemble mean of five ensemble members (*dark gray*). The *gray shading* marks the period between $t = 125$ and $t = 200$ used for the anomalies plotted in Fig. 7. As an indicator of the event duration, *black barcodes* indicate where

the 21-year average of the five ensemble members is larger (**b, e**), respectively smaller (**a, c, d, f**), than the control climate between $t = 0$ and $t = 100$ with 95% confidence using a two-tailed t test. The separate ensemble members are lined up with the start of the perturbation as a tie-point. As a result, the control climate shows a repetition pattern that is caused by the fact that each ensemble member is started from a 10-year continuation of the control climate (Also in Figs. 8, 9)

cooling (Fig. 7a), convection depth decreases (Fig. 7b) and sea ice expansion (Fig. 7a, b) relative to the perturbation by a freshwater pulse. Especially convection in the Irminger Sea (up to 2.5°C colder), and the Hudson Strait outlet ($1\text{--}1.5^{\circ}\text{C}$ colder) are more affected in the IBP experiment, but also the main convection site north of Scandinavia shows an increased sea-ice cover, accompanied by a southward shift of the convection site.

3.4 Discussion of sensitivity experiments

The initial peaks in sea-ice covers and drop in Greenland summit temperatures (Fig. 5) take place during the iceberg discharge (IBP) and the freshwater release (FWP). In both experiments, the short-lived sea-ice retreat that follows is

associated with a warming, resulting from a shift in convection activity from northwest of Norway to northeast of Iceland. This is also accompanied by a short warm interruption at Greenland Summit. A similar fluctuation is observed in SSS en SST near the Denmark Strait in modeling experiments by Manabe and Stouffer (1995), also occurring after a short massive infusion of freshwater. We attribute the short shift in convection zone to regional water column instability resulting from the fast increase in surface water density as the freshwater release stops. The lack of such a flickering response in the Greenland ice core isotope profiles could indicate that such a short-lived convection-episode northeast of Iceland did not happen in reality.

The IBP experiments show a stronger reduction in NADW production, increased sea-ice cover and lower

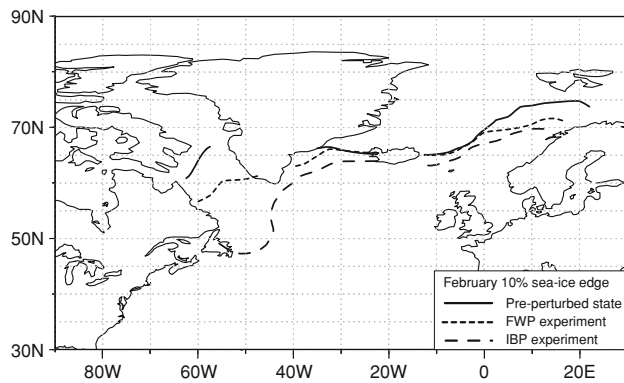


Fig. 6 The level where 10% of sea-ice cover is present in February during the first 10 years after the start of the perturbation (from $t = 100$ to $t = 110$) for the pre-perturbed state (solid line), the FWP scenario (dotted line) and the IBP scenario (hatched line)

Greenland Summit temperatures (Fig. 5) compared to the FWP experiments. As the freshwater volumes of the IBP and FWP experiment are identical, we infer that the additional cooling triggered by the melting icebergs (Fig. 4d) is largely responsible for the increased sea-ice cover in the Northern Hemisphere and associated NADW export reduction (Fig. 5). The spatio-temporal redistribution of the freshwater by icebergs could also play a role, but the response of a sensitivity experiment with non-cooling icebergs resembled that of the FWP experiment (not shown).

The icebergs distribute meltwater over the North Atlantic Ocean, mainly between 40°N and 70°N (Fig. 4c). In this area, the latent heat associated with melting causes a cooling of the surface water of more than 1°C (Fig. 4d). Both the freshwater flux and the latent melting heat facilitate sea-ice formation (Jongma et al. 2009). Sea-ice inhibits deep-water formation through reducing oceanic heat loss to the atmosphere and by reducing sea surface salinity when melting (Wiersma et al. 2006; Bitz et al. 2007) especially in the Irminger Sea and Labrador Sea (Fig. 7a, b). Subsequently, reduced deep-ocean convection and associated reduced northward heat transport maintain the expanded sea-ice cover. Through this positive feedback loop, and because reduced deep-ocean convection slows down the removal of the salinity anomaly (Wiersma et al. 2006), the strongly increased sea-ice cover and reduced deep-ocean convection in the IBP experiment are maintained for up to 100 years after the perturbation (Fig. 7). The cooling caused by the iceberg's latent heat of melting will increase the surface water density, which might be expected to enhance deep convection. In contrast, these results reveal that the deep convection is more affected by the positive feedback of increased sea-ice cover, so that the icebergs melting heat effectively inhibits deep convection.

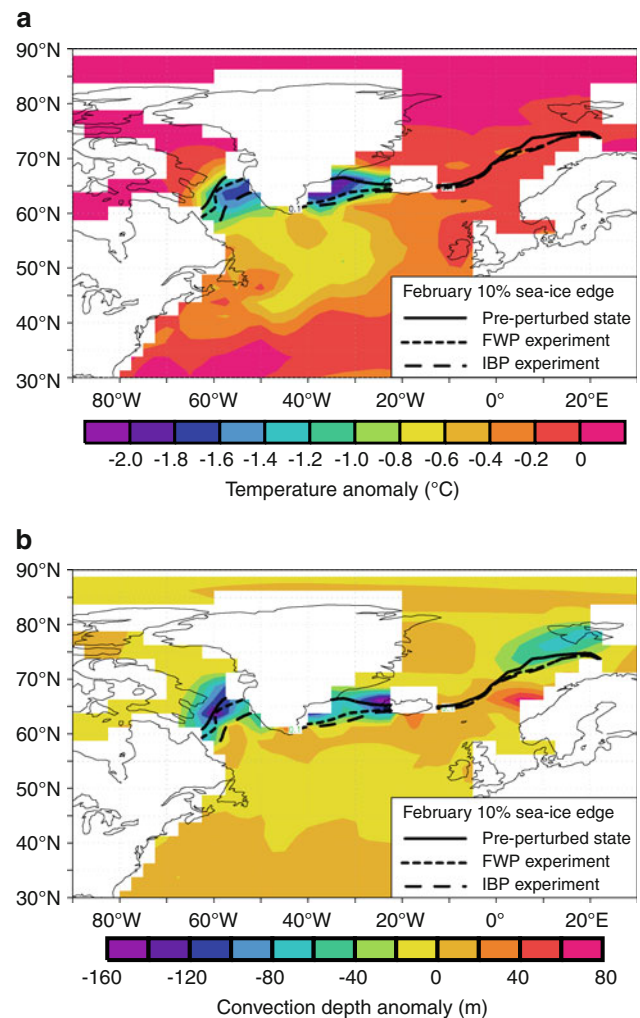


Fig. 7 Anomalies of **a** February SST and **b** February convection depth between the IBP and FWP perturbed states during the interval between years 125 and 200 (as indicated by the shading in Fig. 5). The lines mark the level where 10% of sea-ice cover is present in February during this interval for the pre-perturbed state (solid line), the FWP scenario (dotted line) and the IBP scenario (hatched line)

These findings shed a new light on the 8.2 ka climate event. The catastrophic lake outbursts must have coincided with large iceberg releases if they were accompanied by (partial) collapse of the ice-dam. The discharged icebergs produce a larger weakening in NADW production than a freshwater pulse with the same volume, which is largely due to extra sea-ice facilitation by the latent heat associated with melting icebergs. The effects of sea-ice facilitation and reduced ocean convection are mainly visible in the Labrador Sea and Irminger Sea (Fig. 7). The pronounced cooling in these areas in the IBP experiment also leads to a stronger cooling over central Greenland (Fig. 5c).

We have shown that the cooling caused by melting icebergs can have a significant effect on the ocean circulation response to large perturbations. This could have

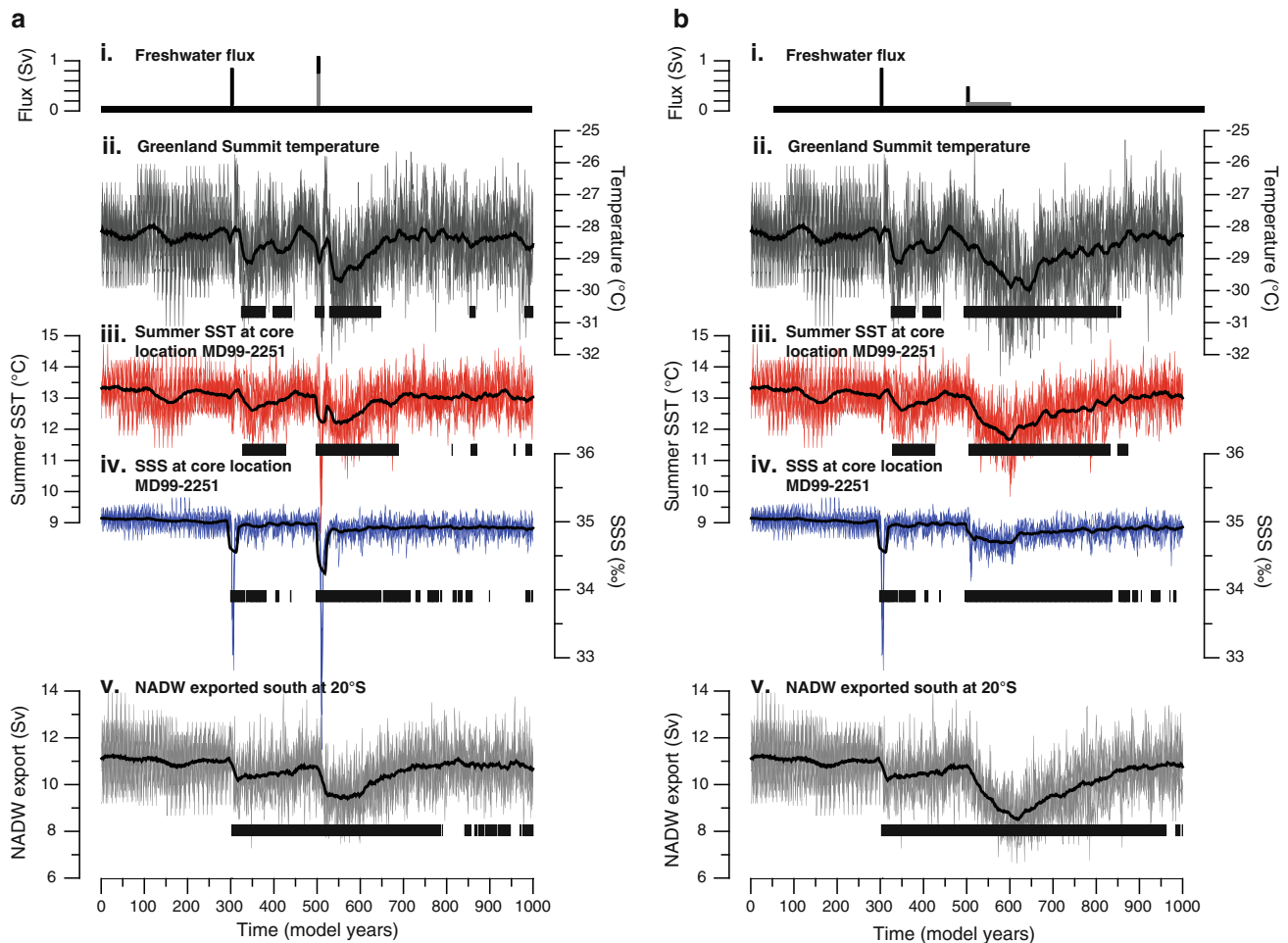


Fig. 8 Simulated surface temperature at the Greenland Summit, surface ocean properties at the location of core MD99-2251 (locations in Fig. 2), and NADW export for two potential drainage scenarios TS-5 (a) and TS-100 (b). The five ensemble members are indicated in gray, with the 21-year running average in black. (i) Freshwater flux (Sv) from freshwater pulses (black) and icebergs (gray) applied in the model. (ii) Simulated surface temperatures from the grid-cell covering the GISP2 and GRIP ice-core location. (iii) Simulated summer SST

from the grid-cell covering deep-ocean sediment core MD99-2251. (iv) Simulated annual SSS from the grid-cell covering MD99-2251. (v) Simulated NADW exported southward in the Atlantic at 20°S. As an indicator of the event duration, *black barcodes* indicate where the 21-year average of the five ensemble members is smaller than the control climate between $t = 200$ and $t = 300$ with 95% confidence using a two-tailed t test

important implications for the simulation of climate events involving large armada's of icebergs, such as Heinrich events.

4 Two-stage lake outburst and ice-dam collapse experiments

4.1 Results

To allow for a data-model comparison between the reconstructed atmospheric and ocean properties (Fig. 1) and the results of the two-stage lake drainage scenarios, we plotted the simulated oceanic response at the coring site of MD99-2251 and the simulated atmospheric response on the

Greenland Summit (Fig. 8). The reconstruction of bottom current strength in MD99-2251 is suggested to reflect changes in large scale overturning intensity (Ellison et al. 2006), and therefore we compare this record to the simulated NADW export. Please keep in mind the difference in time scale and resolution between Figs. 1 and 8. Unless indicated otherwise, the anomalies described here are based on the 21-year running average of the ensemble mean and the duration is estimated from the “barcodes” that indicate the significant anomalies.

The first 500 years of the two-stage lake drainage scenarios (TS-5 and TS-100) are identical. In every ensemble member, sea surface salinity (SSS) at MD99-2251 instantly drops by ~ 2 psu in the individual ensemble members during the first freshwater release (Fig. 8a, b iv) and

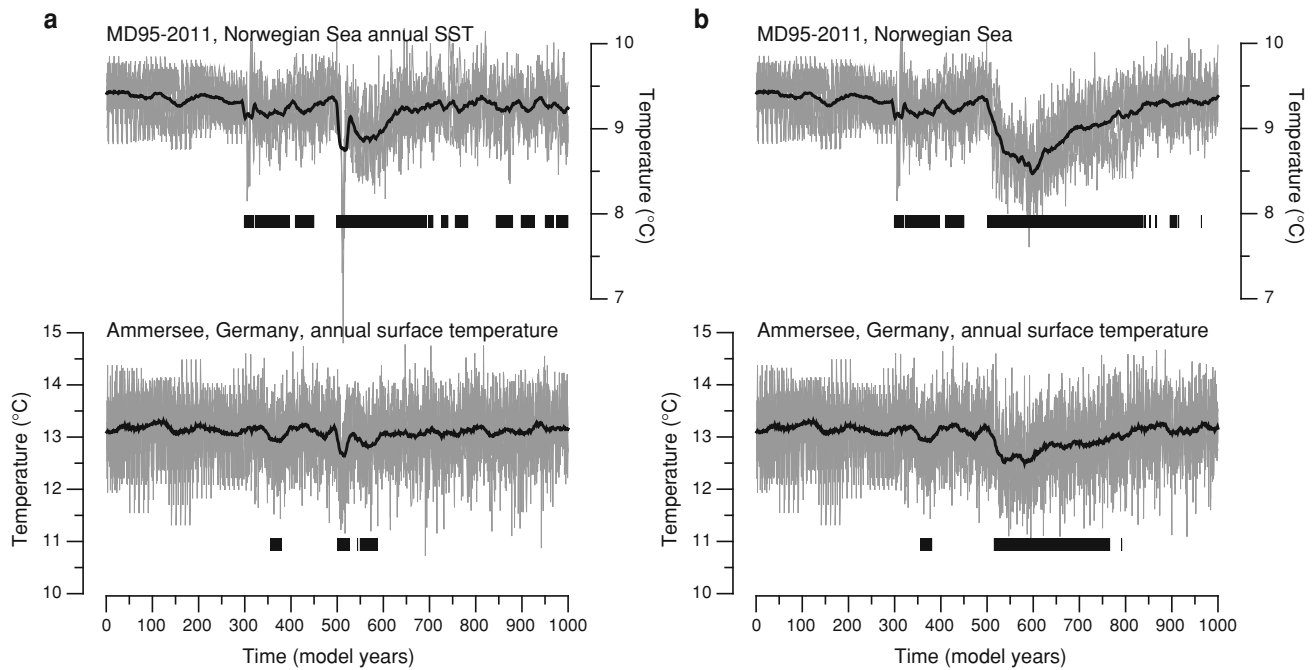


Fig. 9 Five ensemble member (*background lines*) and the 21-year running average of the ensemble mean (*black line*) of simulated annual SSTs over coring site MD95-2011 in the Norwegian Sea and annual surface temperatures over the Ammersee in Germany (locations in Fig. 2) for two potential drainage scenarios TS-5 (a) and TS-

100 (b) (Table 2). The first 500 years are identical. As an indicator of the event duration, *black barcodes* indicate where the 21-year average of the five ensemble members is smaller than the control climate between $t = 200$ and $t = 300$ with 95% confidence using a two-tailed t test

several decades later summer SSTs show a 100-year cooling of $\sim 0.6^\circ\text{C}$ (Fig. 8 a, b iii). The first freshwater pulse causes an at least ~ 200 -year reduction in NADW formation of up to $\sim 10\%$ (Fig. 8a, b v), accompanied by two ~ 50 -year cooling periods of up to 0.8°C over Greenland Summit (Fig. 8a, b ii).

In scenario TS-5 (Table 2), releasing the complete ice-dam volume in icebergs over 5 years together with the second freshwater pulse (Fig. 8a i), results in a short-lived 3.5 psu reduction of ocean surface salinity in the individual ensemble members (Fig. 8a iv). Summer SSTs show an initial drop of 4°C in the individual ensemble members ($\sim 1^\circ\text{C}$ for the 21-year average) coinciding with the freshwater peak at the core location, which is followed by a 190-year cooling period of up to 1°C lower SSTs (Fig. 8a iii). NADW export at 20°S decreases abruptly by 15%, recovering gradually in 300 years (Fig. 8a v). Temperatures over central Greenland are significantly lowered by up to 1.6°C during this same period, briefly interrupted by a relatively warm spike (Fig. 8a ii), that shows similarities to the Icelandic-convection related peak in the sensitivity experiments.

In scenario TS-100 (Table 2) the second freshwater pulse coincides with the start of the 100-years iceberg discharge (Fig. 8b i). SSS decreases by 0.3 psu during the iceberg discharge period of 100 years (Fig. 8b iv), followed by a 240-year period of recovery. The perturbation

leads to a fast reduction in NADW formation of up to 23%, gradually recovering back to pre-perturbed values in about 500 years (Fig. 3b v). Dropping by 1.5°C , SSTs at the core location more or less resemble the NADW trend. Central Greenland temperature responds by a 380-year cooling of up to 2°C (Fig. 8b ii).

To investigate the response on remote locations we plotted the temperature response at the location of Ammersee in Germany (von Grafenstein et al. 1998, 1999) and over deep-ocean sediment core MD95-2011 in the Norwegian Sea (Risebrobakken et al. 2003) (Fig. 9). In these studies, a cooling preceding the “sharp” event is recognized which has been attributed to fluctuations in solar output (Rohling and Pälike 2005). During the “sharp” 8.2 ka climate event, mean annual cooling of respectively ~ 1.7 and $\sim 2.0^\circ\text{C}$ are inferred from proxy data (von Grafenstein et al. 1999; Risebrobakken et al. 2003).

In response to the first freshwater perturbation at $t = 300$, mean annual SSTs in the Norwegian Sea interruptedly drops by up to 0.3°C during a ~ 140 -year period (Fig. 9a, b). Over the Ammersee, this period is characterized by a 20-year cooling of up to 0.3°C . The 5-year perturbation in TS-5 (Table 2) by the second lake drainage and iceberg discharge at $t = 505$ leads to a 210-year cooling of up to 0.7°C over MD95-2011. Over the Ammersee, two cooling periods are simulated within a 100-year period of up to 0.6°C . In TS-100 (Table 2), the

perturbation by the second lake drainage and 100-year iceberg discharge leads to a 350 year cooling of up to 0.9°C over MD95-2011. Over the Ammersee, a 250-year cooling is simulated of up to 0.7°C.

4.2 Discussion of two-stage lake drainage and ice-dam collapse scenarios

The simulated two-stage lake outburst scenario combined with two alternative iceberg discharge scenarios representing the ice-dam collapse is largely consistent with the anomalies observed in the deep-sea core MD99-2251 (Ellison et al. 2006) (Fig. 1): Two distinct cooling events are simulated at the MD99-2251 core location accompanied by two periods of reduced salinity, and overturning decreases in two steps following the lake drainages and ice discharge (Fig. 8a, b). In TS-5 the secondary decrease in NADW export is more abrupt, caused by the rapid sea-ice cover expansion that such an iceberg armada triggers (Fig. 5b), while in scenario TS-100, NADW export gradually decreases during the 100 years of iceberg discharge. The accelerated reduction in NADW formation in both scenarios after the second perturbation may well be promoted by preconditioning of the surface waters by the first perturbation. In TS-100, the steady addition of icebergs triggers an increased sea-ice cover, fresher surface ocean and a gradually weakening overturning circulation. This eventually leads to a stronger climate event than TS-5. Although both scenarios show a NADW response which is in general agreement with the bottom-current strength behavior observed by Ellison et al. (2006), both experiments are lacking the striking overshoot following the weakening in the bottom current strength. This inconsistency may be attributed to the incompatibility between bottom current strength proxy reflecting local bottom current strength and the NADW export parameter from the climate model representing a more universal characteristic.

The simulated cooling following the first lake outburst is widespread. Over Greenland Summit, the cooling is small (0.8°C) when compared with the simulated inter-annual variability at the site, but should be detected in the different Greenland ice core isotope profiles (Dye3, GISP2, GRIP and NorthGRIP). However, no marked cooling is present coinciding with the suggested timing of the lake outburst around 8,470 ka BP (Thomas et al. 2007; Rasmussen et al. 2007). Nevertheless, several other records do show evidence of changes in this period. For instance, a significant increase in dust influx that is interpreted in terms of expansion and intensification of the polar vortex is recorded in the GISP2 ice core around 400 and 200 years before the start of the 8.2 ka climate event (O'Brien et al. 1995; Mayewski et al. 1997). In addition, Rohling and Pälike (2005) report more evidence for a significant climate

change preceding the “sharp” 8.2 ka climate event, such as a decrease in Norwegian Sea summer SST reconstructions in ocean sediment-core MD95-2011 (Risebrobakken et al. 2003), a cooling in Germany (von Grafenstein et al. 1999) and increased aridity in Cariaco Basin (Haug et al. 2001). Simulated temperatures over the Norwegian Sea and the Ammersee do indeed significantly drop following the first lake outburst (Fig. 9).

The second lake outburst combined with the iceberg discharges causes a distinct modeled cooling in Greenland of 1.6°C (TS-5) and 2°C (TS-100) (21-year average of the ensemble mean). In separate ensemble members the lowest decadal average Greenland temperatures in TS-5 and TS-100 is 2.2 and 3.2°C respectively. The magnitude of the TS-100 anomalies is consistent with the reconstructed cooling of $\sim 3.3 \pm 1.1^\circ\text{C}$ (decadal average) during the 8.2 ka climate event in the GISP2 ice core (Kobashi et al. 2007). However, the simulated duration of over 300 years is twice the estimated duration of the 8.2 ka climate event from data. On the other hand, TS-5 shows a duration of anomalies close to observed duration of the 8.2 ka climate event, but might underestimate the magnitude of the event in Greenland, Germany and the Norwegian Sea. The notable absence of a short-lived warm peak in TS-100 might indicate that the slow 100-year iceberg release triggers a more realistic response with regard to convection northeast of Iceland.

In this study we only investigated the impact of a two-stage lake drainage for which evidence is accumulating (e.g., Ellison et al. 2006; Teller et al. 2002; Hillaire-Marcel et al. 2007), combined with ice-dam collapse scenarios. Other modeling studies have pointed to the stochastic nature of the 8.2 ka climate event (Renssen et al. 2002; LeGrande et al. 2006), and these studies have shown that a multiple-stage climate event could also be simulated with a single freshwater pulse. In addition, it has been suggested that single climate forcing (such as a freshwater forcing) could result in climate oscillations occurring on centennial-to millennial time scales (Schulz and Paul 2002; Goosse et al. 2004), or climate oscillations can occur as a function of a minor forcing (Jongma et al. 2007). These studies illustrate that two-stage lake drainage is not required to obtain a two-stage climate event. However, in our model, the different ensemble members exhibit a similar large-scale climate response to a forcing, and neither an important stochastic response is observed, nor a multiple stage event to a single forcing (Wiersma et al. 2006).

Summarizing, our simulations suggest that the first lake outburst could explain the oceanic events recorded in MD99-2251 (Ellison et al. 2006). Although it remains ambiguous that the simulated cooling associated with the first lake outburst is not recorded in the Greenland ice core profiles, the two-stage lake drainage could provide a

solution for the apparent offset in timing between the dated lake outburst and the 8.2 ka climate event in ice cores, provided that the dated red clay-layer in the Hudson Strait was deposited by the first and largest lake drainage (Barber et al. 1999). Accordingly, the simulated first stage lake drainage preceding the “sharp” 8.2 ka climate event might explain the anomalies starting around 8,500 year BP that Rohling and Pälike (2005) report from many records and attribute to fluctuations in solar output, such as Ammersee and MD95-2011. In our idealized simulations discussed in “Sect. 4.1”, the cause for the most pronounced event in Greenland is the collapse of the ice-dam in combination with a small lake outburst, and not a single lake outburst as simulated in other studies (Renssen et al. 2001, 2002; Bauer et al. 2004; Legrande et al. 2006; Wiersma et al. 2006).

The ice-dam has never before been taken into account in hosing experiments for the 8.2 ka climate event, but it may have disappeared in about a 100 years around the event (Dyke 2004). In our experiments, combining a small lake outburst with a 5-year iceberg discharge leads to anomalies with a duration consistent with data, albeit with possibly underestimated amplitudes. A 100-year iceberg discharge leads to more pronounced anomalies, but with too long a duration. In comparison with a freshwater discharge, we have shown that in our model iceberg discharges are more effective in cooling the Greenland Summit (Fig. 5c, f). These results imply that if the ice-dam did indeed disintegrate within a period of 200 years as suggested by reconstructions by Dyke (2004), and was associated with iceberg surges, it probably led to a pronounced cold event in Greenland and the North Atlantic area. Therefore, we tentatively conclude that the single catastrophic lake outburst hypothesis should be revised.

5 Conclusions

We investigated the response of the early Holocene ocean circulation to a perturbation by an iceberg armada released near the Hudson Strait outlet in the ECBilt-CLIO coupled climate model equipped with an interactive iceberg module, and conclude the following:

1. A perturbation by an iceberg discharge leads to more expanded sea-ice cover in the North Atlantic Ocean, a stronger weakening in NADW production, and stronger cooling over Greenland Summit compared to a freshwater perturbation with the same (freshwater) volume.
2. Sea-ice facilitation caused by lower SST resulting from latent heat of melting leads to increased sea-ice

cover in the iceberg discharge experiments. The increased sea-ice cover is responsible for inhibiting convection by reducing oceanic heat loss to the atmosphere and by freshening surface waters when melting. Conversely, the inhibited convection maintains the increased sea-ice cover.

Subsequently, we performed simulations of two-stage lake drainage scenarios for the 8.2 ka climate event in which we accompany the second lake drainage with an iceberg discharge corresponding to the size of the ice-dam that disappeared around the 8.2 ka climate event.

3. A two-stage lake drainage scenario combined with an iceberg discharge representing the collapse of the ice-dam could account for the events recorded in deep-ocean sediment-core MD99-2251 (Ellison et al. 2006) around the 8.2 ka climate event. In addition, it could provide a solution for the apparent offset in timing between the dated lake outburst at 8,470 years BP (Barber et al. 1999) and the start of the event in Greenland at 8,247 years BP (Thomas et al. 2007), and the climate anomalies preceding the 8.2 ka climate event as reported by Rohling and Pälike (2005). However, we note that our scenarios fail to simulate several characteristics in proxy records, such as the lack of a temperature change during the first lake drainage over central Greenland and an overshoot in North Atlantic overturning circulation following the event.
4. Our simulations show that the abrupt 8.2 ka climate event recorded in Greenland could be caused by an iceberg discharge associated with the collapse of the ice-dam in combination with a lake discharge. Accordingly, if the ice-dam did disappear in about a 100 years around the 8.2 ka climate event, it probably led to a pronounced cold event in Greenland and the North Atlantic area.

These results illustrate the importance of latent heat of melting in the simulation of climate events that involve icebergs. Therefore, we recommend that hosing experiments aiming to simulate Heinrich events should take into account the latent heat of melting icebergs.

Acknowledgments This project was sponsored by the Netherlands Organization for Scientific Research. We thank Hans Renssen and Dick Kroon for their comments, and three anonymous reviewers for their helpful reviews.

Open Access This article is distributed under the terms of the Creative Commons Attribution Noncommercial License which permits any noncommercial use, distribution, and reproduction in any medium, provided the original author(s) and source are credited.

References

- Alley RB, Ágústadóttir AM (2005) The 8 k event: cause and consequences of a major Holocene abrupt climate change. *Quat Sci Rev* 24:1123–1149
- Alley RB, Mayewski PA, Sowers T, Stuiver M, Taylor KC, Clark PU (1997) Holocene climatic instability—a prominent, widespread event 8200 yr ago. *Geology* 25(6):483–486
- Barber DC, Dyke A, Hillaire-Marcel C, Jennings AE, Andrews JT, Kerwin MW, Bilodeau G, McNeely R, Southon J, Morehead MD, Gagnon J-M (1999) Forcing of the cold event of 8, 200 years ago by catastrophic drainage of Laurentide lakes. *Nature* 400:344–348
- Bauer E, Ganopolski A, Montoya M (2004) Simulation of the cold climate event 8200 years ago by meltwater outburst from Lake Agassiz. *Paleoceanography*, 19: PA3014. doi:[10.1029/2004PA001030](https://doi.org/10.1029/2004PA001030)
- Berger A (1992) Orbital Variations and Insolation Database. IGBP PAGES/World Data Center-A for Paleoclimatology Data Contribution Series # 92-007., NOAA/NGDC Paleoclimatology Program, Boulder CO, USA
- Berger A, Loutre MF (1991) Insolation values for the climate of the last 10 million years. *Quat Sci Rev* 10(4):297–317
- Bigg GR, Wadley MR, Stevens DP, Johnson JA (1997) Modelling the dynamics and thermodynamics of icebergs. *Cold Reg Sci Technol* 26(2):113–135
- Bitz CM, Chiang JCH, Cheng W, Barsugli JJ (2007) Rates of thermohaline recovery from freshwater pulses in modern, Last Glacial Maximum, and greenhouse warming climates. *Geophys Res Lett* 34: L07708. doi:[10.1029/2006GL029237](https://doi.org/10.1029/2006GL029237)
- Bond G, Showers W, Cheseby M, Lotti R, Almasi P, deMenocal P, Priore P, Cullen H, Hajdas I, Bonani G (1997) A pervasive millennial-scale cycle in North Atlantic Holocene and Glacial climates. *Science* 278:1257–1266
- Bond GC, Kromer B, Beer J, Muscheler R, Evans MN, Showers W, Hoffmann S, Lotti-Bond R, Hajdas I, Bonani G (2001) Persistent solar influence on North Atlantic climate during the Holocene. *Science* 294:2130–2133
- Brovkin V, Bendtsen J, Claussen M, Ganopolski A, Kubatzki C, Petoukhov V, Andreev A (2002) Carbon cycle, vegetation and climate dynamics in the Holocene: experiments with the CLIMBER-2 model. *Global Biogeochem Cycles* 16:1139. doi:[10.1029/2001GB001662](https://doi.org/10.1029/2001GB001662)
- Campin J-M, Goosse H (1999) Parameterization of density-driven downsloping flow for a coarse-resolution ocean model in z-coordinate. *Tellus* 51A:412–430
- Clarke GKC, Leverington DW, Teller JT, Dyke AS (2004) Paleohydrodynamics of the last outburst flood from glacial Lake Agassiz and the 8200 BP cold event. *Quat Sci Rev* 23(3–4):389–407
- Deleersnijder E, Campin J-M (1995) On the computation of the barotropic mode of a free-surface World Ocean model. *Ann Geophys* 13:675–688
- Dowdeswell JA, Whittington RJ, Hodgkins R (1992) The sizes, frequencies and freeboards of East Greenland icebergs observed using ship radar and sextant. *J Geophys Res* 97:3515–3528
- Dyke AS (2004) An outline of North American deglaciation with emphasis on central and northern Canada. In: Ehlers J, Gibbard PL (eds) *Quaternary glaciation—extent and chronology, part II: North America. Developments in quaternary science, vol 2b*. Elsevier, Amsterdam, pp 373–424
- Ellison CRW, Chapman MR, Hall IR (2006) Surface and deep ocean interactions during the cold climate event 8200 years ago. *Science* 312(5782):1929–1932. doi:[10.1126/science.1127213](https://doi.org/10.1126/science.1127213)
- El-Tahan MS, Venkatesh S, El-Tahan H (1987) Validation and quantification assessment of the deterioration mechanisms of Arctic icebergs. *J Offshore Mech Arctic Eng* 109:102–108
- Fichefet T, Morales Maqueda MA (1997) Sensitivity of a global sea ice model to the treatment of ice thermodynamics and dynamics. *J Geophys Res* 102(12):609–646
- Flesche-Kleiven H, Kissel C, Laj C, Ninnemann US, Richter TO, Cortijo E (2008) Reduced North Atlantic deep water coeval with the glacial lake Agassiz freshwater outburst. *Science* 319:60–64
- Ganachaud A, Wunsch C (2000) The ocean meridional overturning circulation, mixing, bottom water formation and heat transport. *Nature* 408:453–457
- Gladstone RM, Bigg GR, Nicholls KW (2001) Icebergs and freshwater fluxes in the Southern Ocean. *J Geophys Res* 106:19903–19915
- Goosse H, Fichefet T (1999) Importance of ice-ocean interactions for the global ocean circulation: a model study. *J Geophys Res* 104:23337–23355
- Goosse H, Masson-Delmotte V, Renssen H, Delmotte M, Fichefet T, Morgan V, van Ommen T, Khim BK, Stenni B (2004) A late medieval warm period in the Southern Ocean as delayed response to external forcing? *Geophys Res Lett* 31(6): L06203. doi:[10.1029/2003GL019140](https://doi.org/10.1029/2003GL019140)
- Haug GH, Hughen KA, Sigman DM, Peterson LC, Rohl U (2001) Southward migration of the intertropical convergence zone through the Holocene. *Science* 293:1304–1308
- Hillaire-Marcel C, de Vernal A, Bilodeau G, Weaver AJ (2001) Absence of deep-water formation in the Labrador Sea during the last interglacial period. *Nature* 410:1073–1077
- Hillaire-Marcel C, de Vernal A, Piper DJW (2007) Lake Agassiz Final drainage event in the northwest Atlantic. *Geophys Res Lett* 34: L15601. doi:[10.1029/2007GL030396](https://doi.org/10.1029/2007GL030396)
- Jakobsson M (2008) The last stampede of a glacial lake. *Nat Geosci* 1:152–153
- Jongma JJ, Prange M, Renssen H, Schulz M (2007) Amplification of interglacial multicentennial climate forcing by mode transitions in North Atlantic overturning circulation. *Geophys Res Lett* 34: L15706
- Jongma JJ, Renssen H, Driesschaert E, Fichefet T, Goosse H (2009) The effect of dynamic-thermodynamic icebergs on the Southern Ocean climate in a three-dimensional model. *Ocean Model* 26:104–113. doi:[10.1016/j.ocemod.2008.09.007](https://doi.org/10.1016/j.ocemod.2008.09.007)
- Josenhans HW, Zevenhuizen J (1990) Dynamics of the laurentide ice sheet in Hudson Bay, Canada. *Mar Geol* 92:1–26
- Kerwin MW (1996) A regional stratigraphic isochron ca. 8000 14C yr B.P from final deglaciation of Hudson Strait. *Quat Res* 46:89–98
- Kobashi T, Severinghaus JP, Brook EJ, Barnola J-M, Grachev AM (2007) Precise timing, characterization of abrupt climate change 8200 years ago from air trapped in polar ice. *Quat Sci Rev* 26:1212–1222. doi:[10.1016/j.quascirev.2007.01.009](https://doi.org/10.1016/j.quascirev.2007.01.009)
- Lajeunesse PG, St-Onge G (2008) The subglacial origin of the lake Agassiz-Ojibway final outburst flood. *Nat Geosci* 1:184–188
- LeGrande AN, Schmidt GA, Shindell DT, Field CV, Miller RL, Koch DM, Faluvegi G, Hoffmann G (2006) Consistent simulations of multiple proxy responses to an abrupt climate change event. *Proc Natl Acad Sci USA* 103(4):837–842
- Leverington D, Mann JD, Teller JT (2002) Changes in bathymetry, volume of glacial lake Agassiz between 9200 and 7700 14C yr BP. *Quat Res* 57:244–252. doi:[10.1006/qres.2001.2311](https://doi.org/10.1006/qres.2001.2311)
- Licciardi JM, Teller JT, Clark PU (1999) Freshwater routing of the Laurentide Ice Sheet during the last deglaciation. In: Clark PU, Webb RS, Keigwin LD (eds) *Mechanisms of global climate change at millennial time scales*. American Geophysical Union, Washington, DC, Geophysical Monograph, 112, 177–201

- Manabe S, Stouffer RJ (1995) Simulation of abrupt climate change induced by freshwater input to the North Atlantic Ocean. *Nature* 378:165–167
- Mayewski PA, Meeker LD, Twickler MS, Whitlow SI, Yang Q, Lyons WB, Prentice M (1997) Major features and forcing of high latitude northern hemisphere atmospheric circulation over the last 110,000 years. *J Geophys Res* 102(C12): 26345–26366
- Moros M, Emeis K, Risebrobakken B, Snowball I, Kuijpers A, McManus J, Jansen E (2004) Sea surface temperatures and ice rafting in the Holocene North Atlantic: climate influences on northern Europe and Greenland. *Quat Sci Rev* 23(20–22):2113–2126
- O'Brien SR, Mayewski PA, Meeker LD, Meese DA, Twickler MS, Whitlow SI (1995) Complexity of Holocene climate as reconstructed from a Greenland ice core. *Science* 270(5244):1962–1964
- Opsteegh JD, Haarsma RJ, Selten FM, Kattenberg A (1998) ECBILT: a dynamic alternative to mixed boundary conditions in ocean models. *Tellus* 50A:348–367
- Peltier WR (1994) Ice age paleotopography. *Science* 265:195–201
- Rasmussen SO, Andersen KK, Svensson AM, Steffensen JP, Vinther BM, Clausen HB, Siggaard-Andersen M-L, Johnsen SJ, Larsen LB, Dahl-Jensen D, Bigler M, Röthlisberger R, Fischer H, Goto-Azuma K, Hansson ME, Ruth U (2006) A new Greenland ice core chronology for the last glacial termination. *J Geophys Res* 111: D06102. doi:[10.1029/2005JD006079](https://doi.org/10.1029/2005JD006079)
- Rasmussen SO, Vinther BM, Clausen HB, Andersen KK (2007) Early Holocene climate oscillations recorded in three Greenland ice cores. *Quat Sci Rev* 26:1907–1914
- Raynaud D, Barnola J-M, Chappellaz J, Blunier T, Indermühle A, Stauffer B (2000) The ice record of Greenhouse gases: a view in the context of future changes. *Quat Sci Rev* 19:9–17
- Renssen H, Goosse H, Fichefet T, Campin J-M (2001) The 8.2 kyr BP event simulated by a global atmosphere–sea-ice–ocean model. *Geophys Res Lett* 28:1567–1570
- Renssen H, Goosse H, Fichefet T (2002) Modeling the effect of freshwater pulses on the early Holocene climate: the influence of high frequency climate variability. *Paleoceanography* 17(2):1020. doi:[10.1029/2001PA000649](https://doi.org/10.1029/2001PA000649)
- Risebrobakken B, Jansen E, Andersson C, Mjelde E, Hevroy K (2003) A high-resolution study of Holocene paleoclimatic and paleoceanographic changes in the Nordic Seas. *Paleoceanography* 18:1017. doi:[10.1029/2002PA000764](https://doi.org/10.1029/2002PA000764)
- Rohling EJ, Pälike H (2005) Centennial-scale climate cooling with a sudden cold event around 8, 200 years ago. *Nature* 434(7036):975–979
- Schulz M, Paul A (2002) Holocene climate variability on centennial-to-millennial time scales: 1. Climate records from the North-Atlantic realm. In: Wefer G, Berger WH, Behre K-E, Jansen E (eds) *Climate development and history of the North Atlantic Realm*. Springer, Berlin, pp 41–54
- Smith SD (1993) Hindcast iceberg drift using current profiles and winds. *Cold Reg Sci Technol* 22:33–45
- Teller JT, Leverington DW, Mann JD (2002) Freshwater outbursts to the oceans from glacial Lake Agassiz and their role in climate change during the last deglaciation. *Quat Sci Rev* 21(8–9):879–887
- Thomas ER, Wolff EW, Mulvaney R, Steffensen JP, Johnsen SJ, Arrowsmith C, White JWC, Vaughn B, Popp T (2007) The 8.2 kyr event from Greenland ice cores. *Quat Sci Rev* 26(1–2):70–81
- von Grafenstein U, Erlenkeuser H, Müller J, Jouzel J, Johnsen S (1998) The cold event 8200 years ago documented in oxygen isotope records of precipitation in Europe and Greenland. *Clim Dyn* 14:73–81
- von Grafenstein U, Erlenkeuser H, Brauer A, Jouzel J, Johnsen SJ (1999) A Mid-European decadal isotope-climate record from 15,500 to 5000 years B.P. *Science* 284:1654–1657
- Watkins SJ, Majer BA, Bigg GR (2007) Ocean circulation at the Last Glacial Maximum: a combined modeling and magnetic proxy-based study. *Palaeoceanography* 22: PA2204. doi:[10.1029/2006PA001281](https://doi.org/10.1029/2006PA001281)
- Weeks WF, Campbell WJ (1973) Icebergs as a fresh water source: an appraisal. *J Glaciol* 12(65):207–233
- Weeks WF, Mellor M (1978) Some elements of iceberg technology. In: Hussein AA (ed) *International Conference and workshop on iceberg utilisation for fresh water production*. Iowa State University, 45–98
- Wiersma AP, Renssen H (2006) Model-data comparison for the 8.2 ka BP event confirmation of a forcing mechanism by catastrophic drainage of Laurentide Lakes. *Quat Sci Rev* 25:63–88
- Wiersma AP, Renssen H, Goosse H, Fichefet T (2006) Evaluation of different freshwater forcing scenarios for the 8.2 ka BP event in a coupled climate model. *Clim Dyn* 27(7–8):831–849. doi:[10.1007/s00382-006-0166-0](https://doi.org/10.1007/s00382-006-0166-0)